Research Square

Preprints are preliminary reports that have not undergone peer review.
They should not be considered conclusive, used to inform clinical practice,
or referenced by the media as validated information.

AI-based MRI brain parcellation reveals region-specific structural remodeling after glioma resection: a longitudinal paired-imaging cohort study

Nigora M. Djuraeva

nodira.bakieva2221@gmail.com

Tashkent State Medical University

Adham I. Ikramov

Khanum V. Abdukhalimova

Mehmet Akşit

Mustafa Fazıl Gelal

Aslı Kahraman

Research Article

Keywords: glioma, artificial intelligence, MRI, brain parcellation, volumetry, neuro-oncology, postoperative remodeling, ventricular system

Posted Date: November 11th, 2026

DOI: https://doi.org/10.21203/rs.3.rs-11323886/v1

License: This work is licensed under a Creative Commons Attribution 4.0 International License.
Read Full License

Additional Declarations: No competing interests reported.

AI-based MRI brain parcellation reveals region-specific structural remodeling after glioma resection: a longitudinal paired-imaging cohort study

Nigora M. Djuraeva, DSc, Professor[1]; Adham I. Ikramov, DSc, Professor[2]; Khanum V. Abdukhalimova, PhD[1]; Mehmet Akşit, MD[3]; Mustafa Fazıl Gelal, MD[3]; Aslı Kahraman, MD[4]

[1] Department of MR and CT, Republican Specialized Scientific and Practical Medical Centre of Surgery named after Academician V. Vakhidov, Tashkent, Uzbekistan

[2] Department of Clinical Radiology, Tashkent Institute for Advanced Medical Studies, Ministry of Health of the Republic of Uzbekistan, Tashkent, Uzbekistan

[3] Department of Radiology, Izmir Katip Celebi University Atatürk Training and Research Hospital, Izmir, Türkiye

[4] Department of Pathology, Izmir Katip Celebi University Atatürk Training and Research Hospital, Izmir, Türkiye

Corresponding author: Nigora M. Djuraeva, DSc, Professor | E-mail: nodira.bakieva2221@gmail.com | ORCID: 0000-0002-2232-8264

ORCIDs: Adham I. Ikramov 0000-0002-7985-7757; Khanum V. Abdukhalimova 0000-0002-2232-8289; Mehmet Akşit 0009-0007-7863-8927; Mustafa Fazıl Gelal 0000-0003-1263-0918; Aslı Kahraman 0000-0001-5781-8506

Abstract

Background: Quantitative postoperative glioma MRI remains predominantly lesion-centered, while structural remodeling of non-tumor brain and cerebrospinal-fluid compartments is incompletely characterized. Methods: We retrospectively analyzed 64 adults with morphologically verified gliomas and technically adequate paired preoperative and postoperative 3D T1-weighted MRI. An automated neural-network Brain Parcellation workflow segmented approximately 110 anatomical regions. Ventricular and CSF volumes were evaluated in the full paired cohort. Whole-brain lobar volumes and interhemispheric asymmetry were additionally assessed in a 30-patient paired subset and compared with 30 demographically comparable healthy controls. Paired tests were selected according to distribution, Hedges' g summarized between-group effects, Spearman correlation assessed associations with tumor diameter, and false-discovery-rate (FDR) correction addressed multiplicity. Results: Right lateral ventricular volume increased from a median 5.11 to 6.29 mL (P=0.03), third ventricular volume from 0.80 to 0.87 mL (P=0.03), and fourth ventricular volume from 1.80 to 2.00 mL (P<0.05), while total CSF volume remained stable (P=0.38). Postoperative patients had lower parietal (-10.7%; g=0.53; q=0.002), occipital (-11.2%; g=0.50; q=0.002), and frontal (-8.4%; g=0.41; q=0.011) volumes than controls. Temporal volume was not significantly different (-3.8%; q=0.35), but temporal asymmetry differed strongly (mean asymmetry index 0.092 vs -0.003; g=-0.55; q=0.001). Tumor diameter showed no FDR-significant association with lobar, asymmetry, or ventricular measures. Conclusions: Automated MRI parcellation identified heterogeneous postoperative remodeling characterized by selective ventricular change, region-specific lobar differences, and persistent temporal asymmetry. Whole-brain quantitative morphometry may complement residual-tumor assessment, although external validation is required.

Keywords: glioma; artificial intelligence; MRI; brain parcellation; volumetry; neuro-oncology; postoperative remodeling; ventricular system

1. Introduction

Maximal safe resection is a central component of glioma management [2–5,13], but the structural consequences of surgery extend beyond the resection cavity. Tumor mass effect, perifocal edema, ventricular compression, tissue displacement, resection, and subsequent decompression can alter the geometry of both parenchymal and cerebrospinal-fluid compartments. Routine postoperative interpretation, however, remains centered primarily on residual enhancing or FLAIR-abnormal tumor and complications.

Automated MRI segmentation provides an opportunity to quantify these changes reproducibly [7–11,16]. Contemporary AI volumetry has demonstrated value for longitudinal glioma assessment and can markedly reduce segmentation time, but most published work has concentrated on tumor burden, response classification, or extent of resection. Whole-brain regional remodeling after tumor removal remains less well characterized, particularly using paired pre-/postoperative imaging combined with ventricular morphometry and interhemispheric asymmetry. Consensus recommendations also describe advanced perfusion imaging methodology [12].

Post-resection morphology is clinically relevant because substantial spatial and network changes can occur after surgery [17–20]. Such changes may affect interpretation of follow-up MRI, radiotherapy planning, functional-anatomical relationships, and the distinction between expected decompression and pathologic ventricular change. A quantitative framework that captures both ventricular and lobar remodeling may therefore add information not represented by tumor diameter or residual volume alone. Advanced imaging contributes to glioma radiotherapy planning [14], while tractography can assist functional pathway preservation [15].

The present study used an automated neural-network Brain Parcellation workflow to quantify ventricular, CSF, lobar, and asymmetry measures in patients undergoing glioma surgery. We hypothesized that postoperative remodeling would be region-specific, would differ from healthy anatomy in selected lobes, and would be more strongly related to tumor topography and mass effect than to tumor size alone. The principal scientific contribution is the integration of paired ventricular morphometry with whole-brain lobar and asymmetry analysis in a single perioperative imaging framework.

2. Materials and Methods

2.1 Study design and participants

This retrospective observational imaging study was conducted at the V. Vakhidov Republican Specialized Scientific-Practical Medical Center of Surgery, Tashkent, Uzbekistan, during 2022–2026. The dissertation cohort contained 70 patients with gliomas for the clinical-morphologic module. Six examinations were excluded from the Brain Parcellation module because MRI quality did not satisfy the predefined volumetric criteria, leaving 64 patients with paired preoperative and postoperative MRI. For the whole-brain lobar comparison, 30 patients with paired MRI were analyzed against 30 healthy volunteers.

Eligibility for automated parcellation required complete whole-brain 3D T1-weighted imaging with isotropic 1×1×1-mm voxels, adequate coverage of both hemispheres, and absence of material motion or metallic artifact. The paired cohort was balanced by tumor laterality (32 right, 32 left); tumor localization was frontal in 41 (64.1%), temporal in 17 (26.6%), and parietal in 6 (9.4%) patients. Patient age in the paired cohort ranged from 45 to 72 years.

2.2 MRI acquisition

MRI was performed at 3.0 T using a Siemens MAGNETOM Vida system with a 64-channel head coil. The broader dissertation protocol included 3D T1-weighted MPRAGE before and after contrast, 3D T2-FLAIR, T2-weighted imaging, DWI/ADC, susceptibility-weighted imaging, perfusion imaging, spectroscopy, DTI/tractography, and functional MRI when clinically indicated. Automated parcellation was based on quality-controlled isotropic 3D T1-weighted data. Standardized brain-tumor imaging protocols inform acquisition and longitudinal interpretation [1].

2.3 Automated Brain Parcellation

Automated segmentation used the CINet-based Brain Parcellation environment (United Imaging Intelligence, China), which segments 110 anatomical subregions. Outputs were aggregated into lobar and ventricular compartments. Ventricular analysis included left and right lateral ventricles, third and fourth ventricles, and total CSF. Interhemispheric asymmetry for paired structures was calculated as (Volume_right - Volume_left)/(Volume_right + Volume_left).

2.4 Imaging endpoints

The primary imaging endpoints were paired change in ventricular volumes and postoperative differences in lobar volumes relative to healthy controls. Secondary endpoints included interhemispheric asymmetry, associations between tumor size and regional measures, and descriptive evaluation of tumor topography/mass-effect patterns. The analysis was intentionally focused on quantitative structural remodeling rather than diagnostic classification performance.

2.5 Statistical analysis

Distributional assumptions were evaluated using the Shapiro-Wilk test and, for samples >50, the Kolmogorov-Smirnov test. Paired continuous variables were analyzed with paired t tests or Wilcoxon signed-rank tests as appropriate. Between-group comparisons were summarized with Hedges' g. Spearman correlation was used for associations involving tumor size and morphometric variables. Multiple comparisons were controlled using the false discovery rate (FDR), with $q<0.05$ considered statistically significant. Analyses in the dissertation were performed using IBM SPSS Statistics 27.0, R 4.3.0, and Python 3.11.

2.6 Ethics

The retrospective AI-based MRI volumetry project was reviewed by the Ethics Committee of Urgench State Medical Institute (approval reference No. 23575432354ref). The available ethics documentation specifies retrospective analysis of de-identified clinical and MRI data and a waiver of written informed consent for use of existing data. The study was conducted in accordance with the Declaration of Helsinki and applicable institutional and national requirements. The archived approval certificate describes the original 60-participant imaging module; institutional confirmation of coverage of the expanded 64-patient parcellation analysis should be retained with the submission records.

3. Results

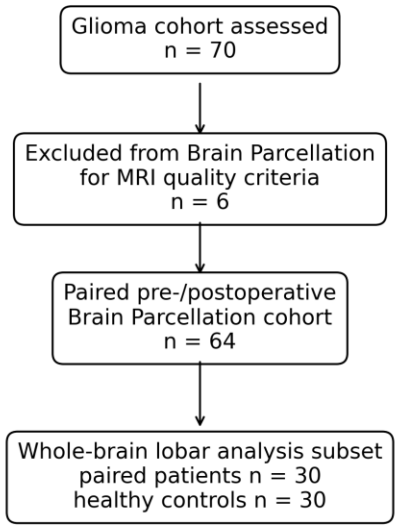
3.1 Cohort and tumor characteristics

Of 70 glioma patients in the relevant dissertation module, 64 (91.4%) met MRI quality requirements for paired Brain Parcellation. Tumor laterality was exactly balanced. Frontal tumors predominated, and half of lesions measured 3.1–5.0 cm.

Baseline cohort characteristics are summarized in Table 1. *[Insert Table 1 here]*

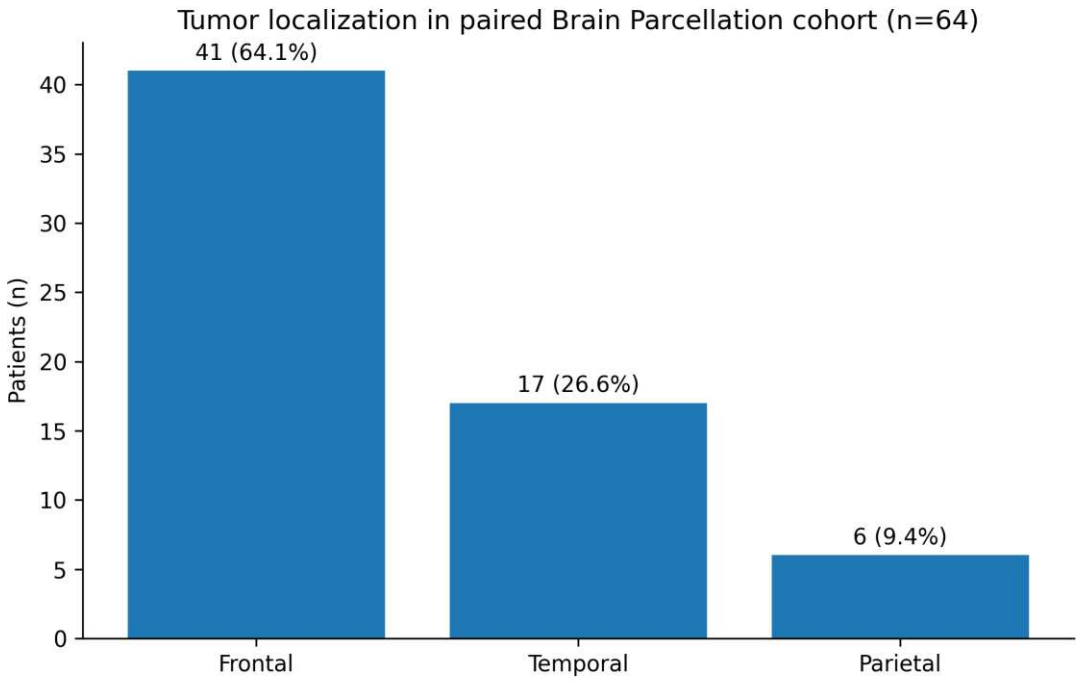
Table 1. Characteristics of the paired Brain Parcellation cohort (n=64)

Characteristic	n	%
Right hemisphere	32	50.0
Left hemisphere	32	50.0
Frontal	41	64.1
Temporal	17	26.6
Parietal	6	9.4
Medial location	39	60.9
Tumor 2.0–3.0 cm	18	28.1
Tumor 3.1–5.0 cm	32	50.0
Tumor >5.0 cm	14	21.9



The cohort selection and analysis flow are shown in Fig. 1. *[Insert Fig. 1 here]*

Figure 1. Study flow for the Brain Parcellation and whole-brain lobar analyses.



The anatomical distribution of tumor locations is shown in Fig. 2. *[Insert Fig. 2 here]*

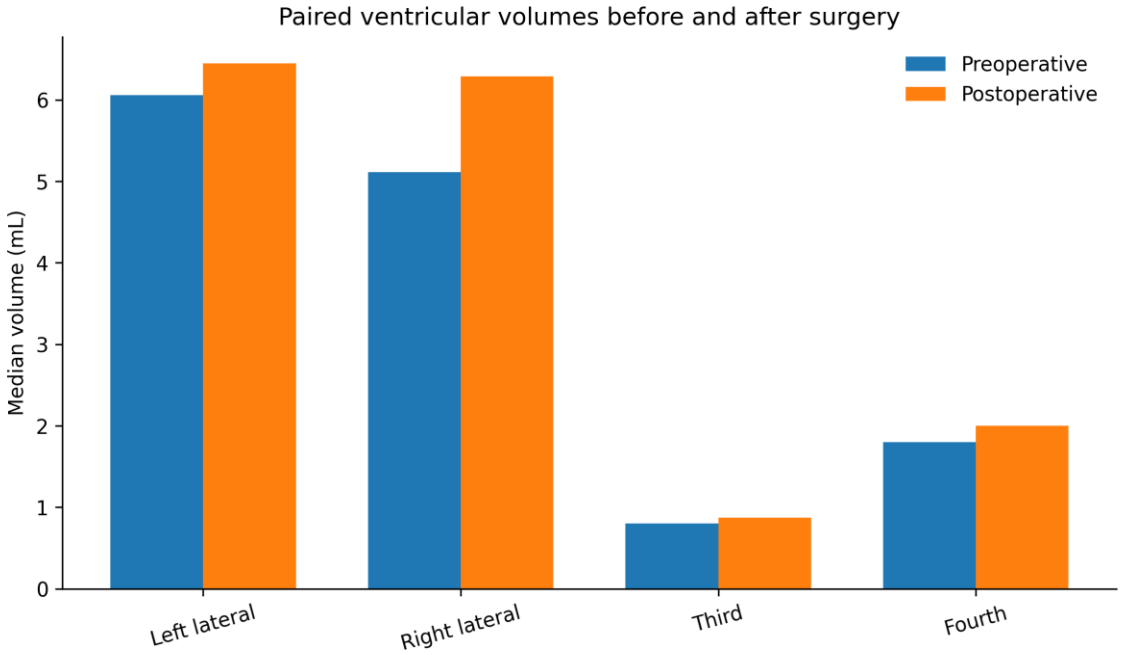
Figure 2. Tumor localization in the paired Brain Parcellation cohort.

3.2 Paired ventricular remodeling

Across the 64 paired examinations, the right lateral, third, and fourth ventricles increased significantly after surgery, whereas the left lateral ventricle showed a borderline increase. The global lateral-ventricular asymmetry index and total CSF volume remained stable. This pattern is consistent with localized postoperative geometric decompression rather than diffuse hydrocephalus.

Table 2. Ventricular and CSF volumes before and after surgery (n=64)

Measure	Preoperative median [Q1;Q3], mL	Postoperative median [Q1;Q3], mL	p
Left lateral ventricle	6.06 [3.86;10.71]	6.45 [4.18;12.34]	0.06
Right lateral ventricle	5.11 [3.73;9.78]	6.29 [4.63;11.39]	0.03
Asymmetry index	0.07 [-0.19;0.34]	0.00 [-0.30;0.55]	0.27
Third ventricle	0.80 [0.52;1.12]	0.87 [0.58;1.36]	0.03
Fourth ventricle	1.80 [1.46;2.26]	2.00 [1.49;2.43]	<0.05
Total CSF	286.1 [256.4;319.2]	286.8 [257.8;323.2]	0.38



Paired ventricular volume distributions are illustrated in Fig. 3. *[Insert Fig. 3 here]*

Figure 3. Median ventricular volumes before and after surgery. Inferential testing used paired distribution-appropriate tests; see Table 2.

3.3 Frontal-tumor mass-effect patterns

Frontal tumors accounted for 41/64 cases. Their mean diameter was 3.79±1.23 cm and increased to 4.77±1.43 cm when perifocal edema was included; tumor and tumor-plus-edema diameters were strongly correlated (r=0.85, p<0.001). Medial frontal tumors (25/41; 61.0%) were larger than lateral tumors (mean 4.00 vs 3.48 cm) and had greater edema-inclusive diameter (5.04 vs 4.35 cm). The dissertation's stratified analysis showed little ventricular change for small frontal tumors, but pronounced remodeling in larger lesions with mass effect.

The exploratory ventricular findings for small frontal tumors are presented in Table 3. *[Insert Table 3 here]*

Table 3. Ventricular change in small frontal tumors (≤3 cm)

Measure	Preoperative mean±SD	Postoperative mean±SD	ΔV	p
Left lateral	11.76±0.77	11.86±0.84	+0.10	0.086
Right lateral	12.74±0.77	12.69±0.83	-0.05	0.781
Third	0.89±0.11	0.89±0.08	≈0	0.960
Fourth	3.18±0.46	3.16±0.38	-0.03	0.720
Total CSF	326.67±11.27	330.15±9.65	+3.48	0.047

The exploratory ventricular findings for large medial frontal tumors with edema are presented in Table 4. *[Insert Table 4 here]*

Table 4. Ventricular change in large medial frontal tumors with marked perifocal edema

Measure	Preoperative	Postoperative	ΔV mean±SD	p

	mean±SD	mean±SD		
Left lateral	16.19±1.05	13.85±1.01	-2.35±0.51	<0.001
Right lateral	6.36±1.09	5.53±0.92	-0.83±0.37	<0.001
Third	2.32±0.66	2.08±0.59	-0.24±0.11	<0.001
Fourth	2.60±0.63	1.86±0.40	-0.74±0.47	0.003
Total CSF	299.35±34.61	235.82±29.94	-63.53±19.51	<0.001

The exploratory ventricular findings for larger frontal tumors without marked edema are presented in Table 5. *[Insert Table 5 here]*

Table 5. Ventricular change in larger frontal tumors without marked edema

Measure	Preoperative mean±SD	Postoperative mean±SD	ΔV mean±SD	p
Left lateral	12.82±1.15	17.51±1.04	+4.69±0.74	0.0001
Right lateral	11.98±1.01	17.83±0.94	+5.85±0.84	<0.0001
Third	1.66±0.22	2.06±0.19	+0.40±0.16	<0.0001
Fourth	1.79±0.12	1.86±0.10	+0.07±0.05	0.0005
Total CSF	347.47±26.22	334.99±26.19	-12.48±7.79	0.0008

Because subgroup denominators were not explicitly reported in the dissertation tables, these stratified results should be interpreted as exploratory and the subgroup n values should be verified against the source dataset before journal submission.

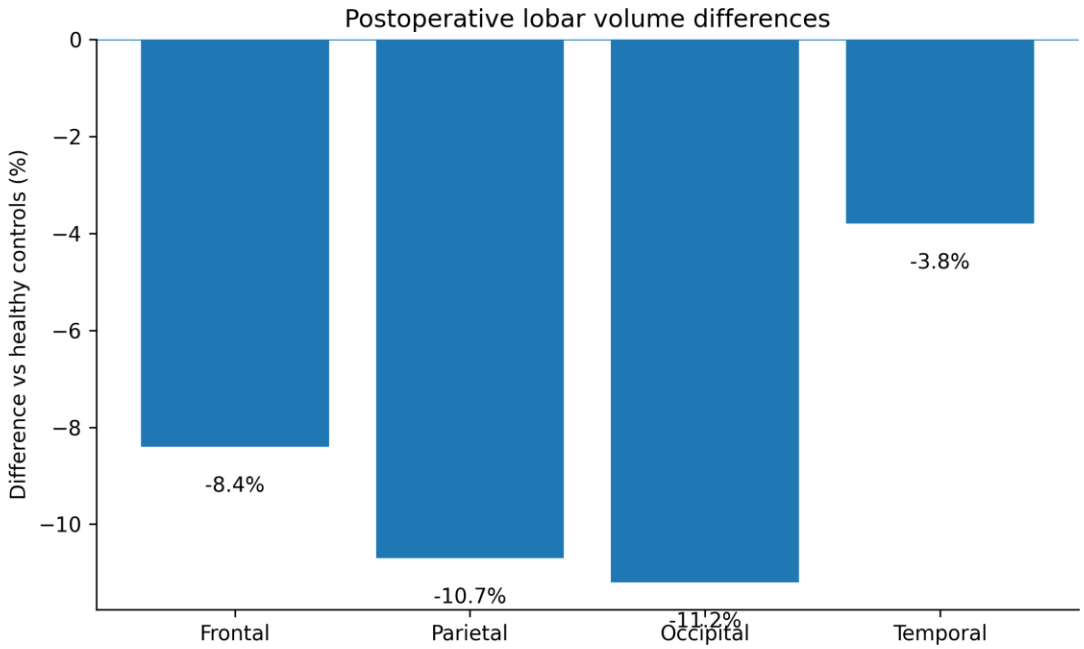
3.4 Whole-brain lobar volumetry

In the whole-brain module, postoperative patients (n=30) were compared with healthy volunteers (n=30). FDR-significant reductions were observed in parietal, occipital, and frontal volumes. The temporal lobe did not show a significant mean-volume difference.

The postoperative and healthy-control lobar volume comparisons are reported in Table 6. *[Insert Table 6 here]*

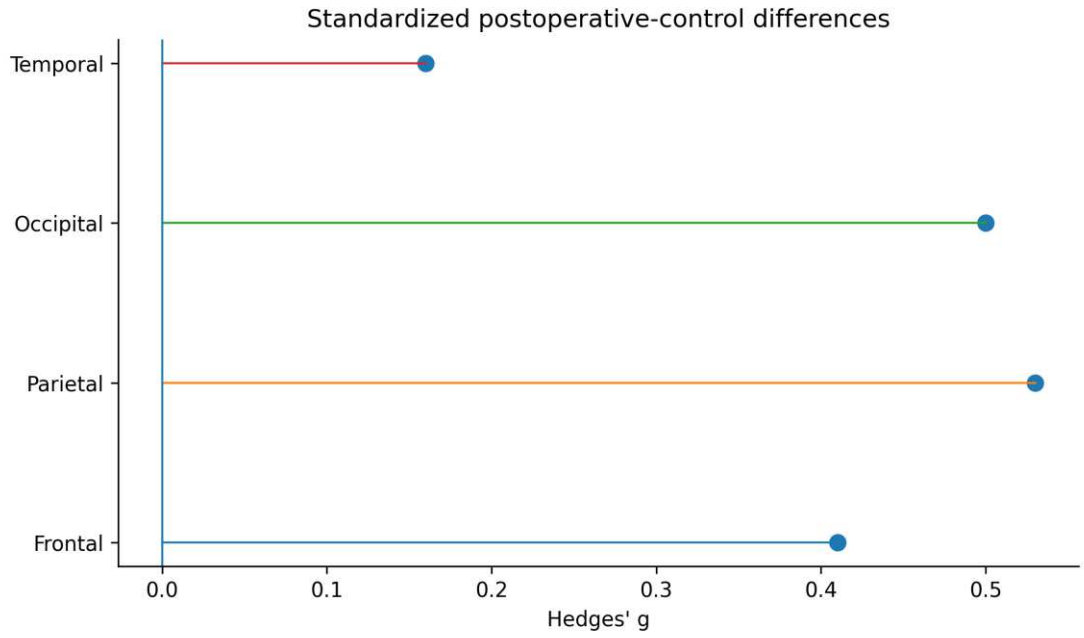
Table 6. Postoperative lobar volumes compared with healthy controls

Region	Postoperative mean, mL	Control mean, mL	Difference	Hedges' g	p	q
Frontal	103.3	112.8	-8.4%	0.41	0.007	0.011
Parietal	109.4	122.6	-10.7%	0.53	0.0005	0.002
Occipital	58.5	65.8	-11.2%	0.50	0.0009	0.002
Temporal	102.9	107.0	-3.8%	0.16	0.30	0.35



The percentage differences in lobar volumes are illustrated in Fig. 4. *[Insert Fig. 4 here]*

Figure 4. Percentage difference in postoperative lobar volume relative to healthy controls.



The standardized effect sizes for the lobar comparisons are illustrated in Fig. 5. *[Insert Fig. 5 here]*

Figure 5. Standardized effect sizes for postoperative-control lobar comparisons.

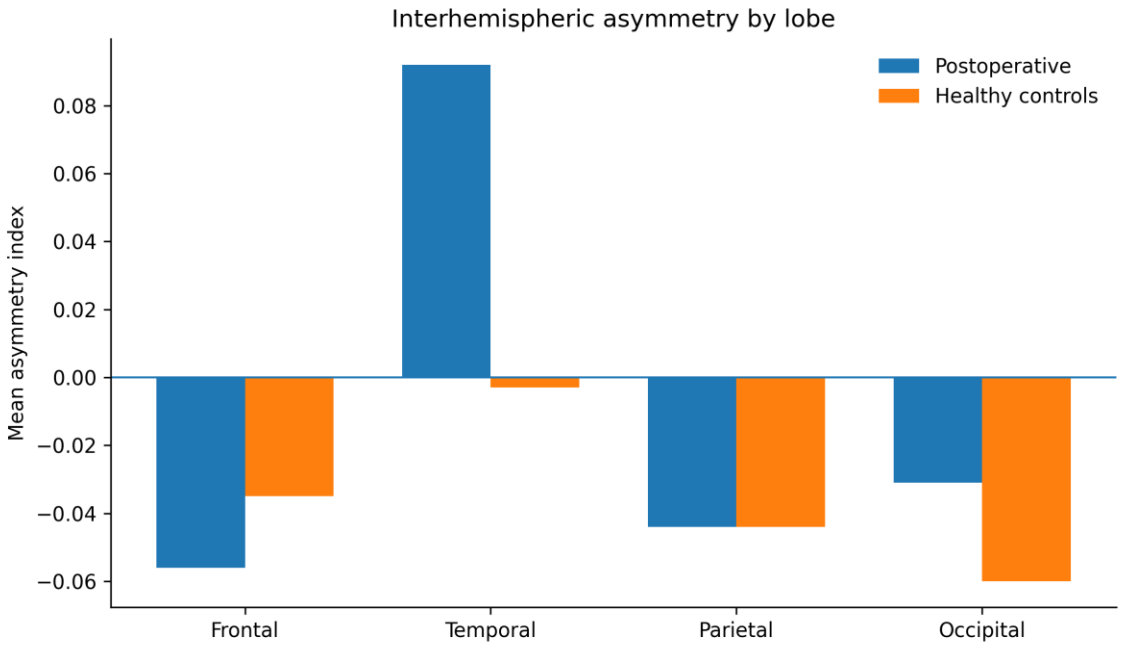
3.5 Interhemispheric asymmetry

Temporal asymmetry was the only lobar asymmetry measure that remained significant after FDR correction. The finding is notable because mean temporal volume was not significantly different, indicating that regional imbalance may capture a postoperative phenotype not visible in bilateral aggregate volume.

Interhemispheric asymmetry results are presented in Table 7. *[Insert Table 7 here]*

Table 7. Lobar asymmetry indices in postoperative patients and healthy controls

Region	Postoperative AI	Control AI	Hedges' g	p	q
Frontal	-0.056	-0.035	0.12	0.42	0.56
Temporal	+0.092	-0.003	-0.55	0.000284	0.001
Parietal	-0.044	-0.044	0.06	0.70	0.70
Occipital	-0.031	-0.060	-0.19	0.22	0.43



The lobar asymmetry indices are illustrated in Fig. 6. *[Insert Fig. 6 here]*

Figure 6. Mean interhemispheric asymmetry indices by lobe.

3.6 Relationship with tumor size

After FDR correction, tumor size was not significantly associated with lobar volume, asymmetry, or ventricular morphometry. A nominal association with temporal volume (Spearman r=0.43, p=0.018) did not survive multiplicity correction (q=0.092).

Correlations between tumor size and lobar measures are summarized in Table 8. *[Insert Table 8 here]*

Table 8. Correlation between tumor size and lobar morphometry

Parameter	Spearman r	p	q
Frontal volume	0.09	0.65	0.65
Temporal volume	0.43	0.018	0.092
Parietal volume	0.31	0.099	0.247
Occipital volume	0.24	0.195	0.326
Frontal AI	-0.02	0.91	0.91
Temporal AI	-0.28	0.129	0.515
Parietal AI	-0.07	0.73	0.91

Occipital AI	0.10	0.59	0.91

Correlations between tumor size and ventricular measures are summarized in Table 9. *[Insert Table 9 here]*

Table 9. Correlation between tumor size and ventricular morphometry

Parameter	Spearman r	p	q
Third-ventricle width	-0.10	0.60	0.68
Frontal-horn width	-0.27	0.15	0.48
Third-ventricle volume	-0.08	0.68	0.68
Fourth-ventricle volume	+0.17	0.36	0.48
Inferior lateral ventricle, left	+0.27	0.15	0.48
Inferior lateral ventricle, right	+0.25	0.18	0.48
Lateral ventricle, left	+0.21	0.25	0.48
Lateral ventricle, right	+0.19	0.32	0.48

4. Discussion

The principal novelty is the integrated perioperative assessment of non-tumor brain remodeling rather than AI segmentation itself. By combining paired ventricular/CSF morphometry, lobar volumetry, hemispheric asymmetry, and topographic mass-effect analysis, the study tests whether postoperative anatomy contains quantitative information not captured by residual-tumor volume or tumor diameter alone.

This study demonstrates that automated whole-brain MRI parcellation can characterize postoperative structural change after glioma resection at several anatomical scales. Three findings are central. First, ventricular remodeling was selective rather than global: the right lateral, third, and fourth ventricles increased while total CSF remained stable. Second, postoperative patients showed FDR-significant differences in frontal, parietal, and occipital lobar volumes compared with healthy controls. Third, temporal asymmetry persisted despite a non-significant difference in total temporal volume, suggesting that asymmetry may provide information distinct from bilateral volume.

The scientific significance lies in moving postoperative volumetry beyond the tumor itself. Recent AI-based glioma studies have established the feasibility and efficiency of automated tumor-volume measurement [16,23–25], while other MRI work demonstrates that resection can produce substantial postoperative morphologic and network changes [17–20,22]. The present analysis extends that concept to non-tumor brain compartments by jointly examining ventricular geometry, lobar volume, and hemispheric asymmetry.

The ventricular findings should not be interpreted as simple hydrocephalus. Total CSF did not change significantly, and the pattern varied according to frontal tumor mass effect. This supports a model of local decompression and geometric redistribution. The strong correlation between tumor diameter and edema-inclusive diameter, together with the more pronounced mass effect of medial frontal lesions, provides an anatomical explanation for why topography may matter more than absolute tumor size.

The lobar analysis also argues against a uniform postoperative brain-volume response. Parietal and occipital differences were numerically largest, followed by frontal volume, whereas temporal volume was relatively preserved. At the same time, temporal asymmetry was the strongest asymmetry signal. A plausible interpretation is that bilateral aggregate volume and interhemispheric balance reflect different

components of postoperative anatomy; the latter may be sensitive to unilateral displacement, resection, or compensatory reorganization.

Clinically, quantitative parcellation could complement conventional postoperative MRI in three ways: documenting expected decompression, identifying regional structural imbalance that may merit longitudinal follow-up, and providing objective anatomical covariates for studies of neurological outcome, cognitive recovery, and radiotherapy planning. These uses remain hypothesis-generating in the present study and require prospective validation before individual-patient decision thresholds can be recommended.

These observations are consistent with an expanding morphometric and network literature showing that glioma-related structural change extends beyond the visible lesion [18–22]. A 2025 systematic review of MRI morphometry identified both contralesional gray-matter increase and atrophy across glioma studies, emphasizing dependence on tumor location, grade, and individual anatomy. More recent work has linked contralesional gray-matter volume to postoperative cognition and has demonstrated surgery-associated disruption and compensatory plasticity using multimodal MRI. Together, these studies support interpreting regional volume and asymmetry as distributed markers of tumor- and treatment-related brain reorganization rather than simple surrogates of resection volume.

The study has limitations. It is retrospective and single-center. The paired Brain Parcellation cohort was modest, and the whole-brain comparison used a smaller 30-patient subset. Timing of postoperative MRI, histomolecular subgroup distributions, extent of resection, and postoperative therapy were not incorporated into the present morphometric models. The healthy comparison was demographically comparable but not a longitudinal within-person control. Subgroup denominators for the exploratory frontal mass-effect tables must be verified from the source dataset. Finally, automated segmentation in postoperative brains can be challenged by resection cavities and distorted anatomy; future work should include formal segmentation-quality metrics and external validation.

Future studies should prospectively pair parcellation outputs with WHO CNS5 molecular class, IDH status, extent of resection, edema volume, neurological and cognitive outcomes, and serial postoperative time points. Multicenter external validation would determine whether the regional patterns observed here are reproducible across scanners, segmentation platforms, and surgical strategies. The evolving role of neuronavigation provides an additional context for integrating quantitative imaging into surgical workflows [26].

5. Conclusions

AI-based Brain Parcellation identified region-specific structural remodeling after glioma surgery. Postoperative changes involved selective ventricular expansion with stable total CSF, lower frontal/parietal/occipital volumes relative to healthy controls, and persistent temporal asymmetry. The absence of FDR-significant correlations with tumor size supports a topography- and mass-effect-dependent model rather than a size-only model. Quantitative whole-brain morphometry warrants prospective validation as a complementary postoperative imaging biomarker.

AI, artificial intelligence; CSF, cerebrospinal fluid; FDR, false discovery rate; MRI, magnetic resonance imaging; MPRAGE, magnetization-prepared rapid gradient echo.

Abbreviations

Declarations

Authors' information

Not applicable.

Acknowledgements

Not applicable.

Authors' contributions

NMD conceived the study, supervised the imaging work, interpreted the findings, and contributed to manuscript drafting. AII contributed to study design, radiologic interpretation, and critical revision. KVA contributed to data curation, imaging analysis, and manuscript revision. MA and MFG contributed to radiologic interpretation, methodological review, and critical revision. AK contributed to pathologic interpretation and critical revision. All authors read and approved the final manuscript. Authors should verify these CRediT-equivalent statements before submission.

Funding

No external funding was documented for the study in the source materials used to prepare this manuscript.

Competing interests

The authors declare that they have no competing interests.

Availability of data and materials

The de-identified dataset supporting the findings is not publicly available because of participant privacy and institutional data-governance restrictions. De-identified data may be available from the corresponding author on reasonable request and subject to approval by the relevant institution and ethics/data-protection requirements.

Consent for publication

Not applicable. No identifiable individual participant information is reported.

Ethics approval and consent to participate

The retrospective AI-based MRI volumetry project was reviewed by the Ethics Committee of Urgench State Medical Institute (approval reference No. 23575432354ref). The available approval documentation specifies a waiver of written informed consent for retrospective use of existing de-identified clinical and MRI data. The study was conducted in accordance with the Declaration of Helsinki. Institutional confirmation of coverage of the expanded 64-patient parcellation analysis should be retained with the submission records.

References

1. Ellingson BM, Bendszus M, Boxerman J, et al. Consensus recommendations for a standardized Brain Tumor Imaging Protocol in clinical trials. Neuro Oncol. 2015;17:1188–1198.

2. Louis DN, Perry A, Wesseling P, et al. The 2021 WHO Classification of Tumors of the Central Nervous System: a summary. Neuro Oncol. 2021;23:1231–1251.

3. WHO Classification of Tumours Editorial Board. Central Nervous System Tumours. WHO Classification of Tumours. 5th ed. Lyon: International Agency for Research on Cancer; 2021.

4. Weller M, van den Bent M, Preusser M, et al. EANO guidelines on the diagnosis and treatment of diffuse gliomas of adulthood. Nat Rev Clin Oncol. 2021;18:170–186.

5. Wen PY, Weller M, Lee EQ, et al. Glioblastoma in adults: a Society for Neuro-Oncology and European Society of Neuro-Oncology consensus review. Neuro Oncol. 2020;22:1073–1113.

6. Smits M. MRI biomarkers in neuro-oncology. Nat Rev Neurol. 2021;17:486–500.

7. Henschel L, Conjeti S, Estrada S, et al. FastSurfer—a fast and accurate deep learning based neuroimaging pipeline. NeuroImage. 2020;219:117012.

8. Henschel L, Kügler D, Reuter M. FastSurferVINN: building resolution-independence into deep learning segmentation methods. NeuroImage. 2022;251:118933.

9. Fischl B. FreeSurfer. NeuroImage. 2012;62:774–781.

10. Isensee F, Jaeger PF, Kohl SAA, Petersen J, Maier-Hein KH. nnU-Net: a self-configuring method for deep learning-based biomedical image segmentation. Nat Methods. 2021;18:203–211.

11. Cerri S, Puonti O, Meier DS, et al. A contrast-adaptive method for simultaneous whole-brain and lesion segmentation. NeuroImage. 2021;225:117471.

12. Boxerman JL, Quarles CC, Hu LS, et al. Consensus recommendations for a dynamic susceptibility contrast MRI protocol for use in high-grade gliomas. Neuro Oncol. 2020;22:1262–1275.

13. Patel SH, Bansal AG, Young EB, et al. Extent of surgical resection in lower-grade gliomas: differential impact based on molecular subtype. AJNR Am J Neuroradiol. 2019;40:1149–1155.

14. Castellano A, Bailo M, Cicone F, et al. Advanced imaging techniques for radiotherapy planning of gliomas. Cancers (Basel). 2021;13:1063.

15. Bello L, Gambini A, Castellano A, et al. Motor and language DTI fiber tracking combined with intraoperative subcortical mapping for surgical removal of gliomas. NeuroImage. 2008;39:369–382.

16. Asfaw ZK, Young T, Hernandez Marquez G, et al. Artificial intelligence-based volumetric measurements for longitudinal clinical assessment of treatment response in high-grade gliomas: validation across institutional and public datasets. Neurooncol Adv. 2026;8:vdag045. doi:10.1093/noajnl/vdag045.

17. Cheng R, Hu X, Wang X, Huangfu B, Lan Q. MRI reveals glioma surgery-induced brain network disruption and compensatory plasticity. Neuroscience. 2026;614:296–306. doi:10.1016/j.neuroscience.2026.07.037.

18. Manso-Ortega L, Gisbert-Muñoz S, Amoruso L, et al. Contralesional grey matter volume as an index of macrostructural plasticity in patients with brain tumors. NeuroImage. 2026;337:122029. doi:10.1016/j.neuroimage.2026.122029.

19. Brain MRI morphometry for structural alterations in patients with glioma – a systematic review. Eur J Radiol Open. 2025;14:100660. doi:10.1016/j.ejro.2025.100660.

20. Predictors of cognition after glioma surgery: connectotomy, structure-function phenotype, plasticity. Brain. 2024;147:2621–2635. doi:10.1093/brain/awae093.

21. Isaac MFG. Post-therapy imaging of adult brain tumours: patterns, pitfalls, and practical framework. Insights Imaging. 2026;17:231. doi:10.1186/s13244-026-02398-y.

22. Non-Invasive Measurement of Cortical Plasticity in Brain Tumour Surgery: A Monocentric Experience of nTMS Mapping and Definition of Cognitive Reshaping Based on Tumour Histological Grade. Cancers (Basel). 2026;18:1405.

23. Alhalabi OT, Mironov K, Nabiev K, et al. The utility of intraoperative magnetic resonance imaging in recurrent glioblastoma surgery: a volumetric analysis. Brain Spine. 2026;6:106135.

24. Sadeghi S, Shokatian I, Siavashpour Z, et al. MRI-based gross tumor volume delineation in high-grade glioma using a deep convolutional neural network. Appl Radiat Isot. 2026;236:112797.

25. Bijlsma S, Maal T, Rubbert C, et al. AI radiomics predicts spatial glioma recurrence on preoperative MRI: a systematic review. Eur J Radiol. 2025;193:112412.

26. Sulangi AJ, Husain SF, Liu Y, et al. Neuronavigation in glioma resection: current applications, challenges, and emerging innovations. Front Surg. 2024;11:1430567.